

Benzothiadiazole-Based Linear and Star Molecules: Design, Synthesis, and Their Application in Bulk Heterojunction Organic Solar Cells

Weiwei Li,^{†,‡} Chun Du,[†] Fenghong Li,[‡] Yi Zhou,[‡] Mats Fahlman,[‡] Zhishan Bo,^{*,†} and Fengling Zhang^{*,‡}

[†]Laboratory of Polymer Physics and Chemistry, Institute of Chemistry CAS, Beijing 100190, China, and

[‡]Department of Physics, Chemistry and Biology, Linköping University, SE-58183, Linköping, Sweden

Received August 24, 2009. Revised Manuscript Received September 29, 2009

Star molecules have many advantages, such as monodispersity, excellent solubility, and vast structures with different functional groups. A set of four-arm star molecules with benzothiadiazole as the core, oligothiophene as the arm, and triphenylamine as the end group and their linear counterparts were designed and synthesized. Organic solar cells (OSCs) fabricated with these star molecules and [6,6]-phenyl C₇₁ butyric acid methyl ester (PC₇₁BM) by spin-coating from solution demonstrate similar short circuit current density (J_{sc}) and fill factor (FF) but larger open circuit voltage (V_{oc}) in comparison with solar cells fabricated with corresponding linear molecules and PC₇₁BM. A power conversion efficiency (PCE) of 1.8%, with $J_{sc} = 4.9 \text{ mA/cm}^2$, $V_{oc} = 0.92 \text{ V}$, and $FF = 0.41$ was achieved with one of these star molecules.

Introduction

Polymer solar cells are striking due to their low cost solution process and high power conversion efficiency (PCE).^{1–6} However, the performance of polymer solar cells depends strongly on the purity, the molecular weight, and the molecular weight distribution of polymers. The control of the molecular weight and the molecular distribution of polymers by polymerization and the purification of polymers are usually difficult, which makes it difficult to have reproducible results for solar cell application.⁷ Solar cells based on organic molecules are inferior to polymer solar cells because their active layers are usually deposited via vacuum vapor. Recently, soluble organic molecules were synthesized and utilized in organic solar cells (OSCs).^{8–10} These soluble molecules

are promising materials due to solution processing and the purity of molecules.

Compared with linear conjugated oligomers and polymers used in the opto-electric field, star molecules have a number of advantages.^{11,12} With tailoring functional groups in the core and the arm, star molecules can be designed to realize low band gap, broad absorption, and high mobility for improving power conversion efficiency (PCE) of OSCs and also excellent solubility for low cost solution process.^{13–21} Currently, star molecules have been developed as an interesting class of semiconducting materials and used in OSCs.^{13–21} Roncali et al. first reported a class of new benzotrithiophene-cored star oligothiophenes, which demonstrated semiconducting characteristics for solution processing OSCs with PCE

*E-mail: zsbo@iccas.ac.cn (Z.B.) and fenzh@ifm.liu.se (F.Z.).

- (1) Liang, Y. Y.; Feng, D. Q.; Wu, Y.; Tsai, S. T.; Li, G.; Ray, C.; Yu, L. P. *J. Am. Chem. Soc.* **2009**, *131*, 7792.
- (2) Park, S. H.; Roy, A.; Beaupré, S.; Cho, S.; Coates, N.; Moon, J. S.; Moses, D.; Leclerc, M.; Lee, K.; Heeger, A. J. *Nat. Photon.* **2009**, *3*, 297.
- (3) Svensson, M.; Zhang, F. L.; Veenstra, S. C.; Verhees, W. J. H.; Hummelen, J. C.; Kroon, J. M.; Inganäs, O.; Andersson, M. R. *Adv. Mater.* **2003**, *15*, 988.
- (4) Peet, J.; Kim, J. Y.; Coates, N. E.; Ma, W. L.; Moses, D.; Heeger, A. J.; Bazan, G. C. *Nat. Mater.* **2007**, *6*, 497.
- (5) Wang, E. G.; Wang, L.; Lan, L. F.; Luo, C.; Zhuang, W. L.; Peng, J. B.; Cao, Y. *Appl. Phys. Lett.* **2008**, *92*, 033307.
- (6) Hou, J. H.; Chen, H. Y.; Zhang, S. Q.; Li, G.; Yang, Y. *J. Am. Chem. Soc.* **2008**, *130*, 16144.
- (7) Thompson, B. C.; Fréchet, J. M. J. *Angew. Chem., Int. Ed.* **2008**, *47*, 58.
- (8) Lloyd, M. T.; Anthony, J. E.; Malliaras, G. G. *Mater. Today* **2007**, *10*, 34.
- (9) Walker, B.; Tamayo, A. B.; Dang, X. D.; Zalar, P.; Seo, J. H.; Garcia, A.; Tantiwiwat, M.; Nguyen, T. Q. *Adv. Funct. Mater.* **2009**, *19*, 3063.
- (10) Rousseau, T.; Cravino, A.; Bura, T.; Ulrich, G.; Ziessel, R.; Roncali, J. *Chem. Commun.* **2009**, 1673.

- (11) Li, B. S.; Li, J.; Fu, Y. Q.; Bo, Z. S. *J. Am. Chem. Soc.* **2004**, *126*, 3430.
- (12) Ponomarenko, S. A.; Tatarinova, E. A.; Muzafarov, A. M.; Kirchmeyer, S.; Brassat, L.; Mourran, A.; Moeller, M.; Setayesh, S.; de Leeuw, D. *Chem. Mater.* **2006**, *18*, 4101.
- (13) He, C.; He, Q. G.; Yi, Y. P.; Wu, G. L.; Bai, F. L.; Shuai, Z. G.; Li, Y. F. *J. Mater. Chem.* **2008**, *18*, 4085.
- (14) Ma, C. Q.; Fonrodona, M.; Schikora, M. C.; Wienk, M. M.; Janssen, R. A. J.; Bäuerle, P. *Adv. Funct. Mater.* **2008**, *18*, 3323.
- (15) Fischer, M. K. R.; Ma, C. Q.; Janssen, R. A. J.; Debaerdemaeker, T.; Bäuerle, P. *J. Mater. Chem.* **2009**, *19*, 4784.
- (16) Kopidakis, N.; Mitchell, W. J.; van de Lagemaat, J.; Ginley, D. S.; Rumbles, G.; Shaheen, S. E.; Rance, W. L. *Appl. Phys. Lett.* **2006**, *89*, 103524.
- (17) Lee, T. W.; Kim, D. C.; Kang, N. S.; Yu, J. W.; Cho, M. J.; Kim, K. H.; Choi, D. H. *Chem. Lett.* **2008**, *37*, 866.
- (18) Kim, Y. G.; Christian-Pandya, H.; Ananthakrishnan, N.; Niazimbetova, Z. I.; Thompson, B. C.; Galvin, M. E.; Reynolds, J. R. *Sol. Energ. Mat. Sol. Cells* **2008**, *92*, 307.
- (19) Alévêque, O.; Leriche, P.; Cocherel, N.; Frère, P.; Cravino, A.; Roncali, J. *Sol. Energ. Mat. Sol. Cells* **2008**, *92*, 1170.
- (20) Cravino, A.; Roquet, S.; Alévêque, O.; Leriche, P.; Frère, P.; Roncali, J. *Chem. Mater.* **2006**, *18*, 2584.
- (21) Roncali, J.; Frère, P.; Blanchard, P.; de Bettignies, R.; Turbiez, M.; Roquet, S.; Leriche, P.; Nicolas, Y. *Thin Solid Films* **2006**, *511*, 567.

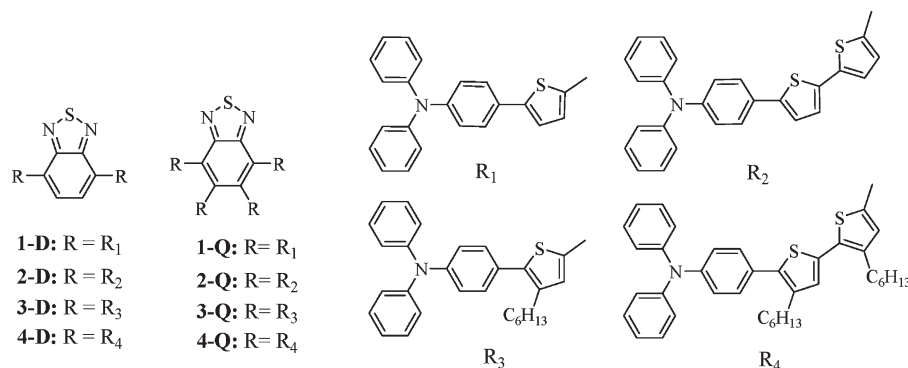


Figure 1. Structure of linear and star molecules.

of 0.78%.²¹ A series of thiophene-based dendrimers^{13–15,22} were also synthesized with PCE up to 1.85%,²² which is the highest efficiency for star molecules until now.

Benzothiadiazole-based low band gap conjugated polymers with main chain donor–acceptor alternating structures have been intensively investigated in OSCs, and a PCE of 6.1% has been reported.^{1–6} Our strategy is to introduce benzothiadiazole into molecules to lower the band gap and increase the PCE of OSCs. In this study, a series of star molecules based on the benzothiadiazole core were synthesized as shown in Figure 1. Functional groups were introduced into four reaction positions 4, 5, 6, and 7 of benzothiadiazole to form star molecules. Compared to star molecules, two-arm linear molecules based on the 4,7-positions of benzothiadiazole were also designed and synthesized. Triphenylamine (TPA) was introduced as the end group for its typical electron donating and hole transporting properties, by which the band gap of molecule would be reduced by internal charge transfer.²³ In the literature, a solution-processable star molecule based on TPA as a central core and benzothiadiazole as an end group has been designed for OSCs with electrochemical bandgap of 2.04 eV and a PCE of 0.61%,²⁴ which implies that the TPA–benzothiadiazole structure is promising for OSCs.

Photovoltaic devices based on blends of these molecules as donor and [6,6]-phenyl C₇₁ butyric acid methyl ester (PC₇₁BM) as acceptor were fabricated by spin-coating and characterized under illumination of a solar simulator. Star molecules demonstrated high V_{oc} compared with corresponding linear molecules due to their low highest occupied molecular orbital (HOMO) levels. For both linear and star molecules, similar J_{sc} and fill factor (FF) values have been obtained, suggesting that their conductivity is comparable. OSCs based on star molecule **3-Q** and PC₇₁BM present the highest PCE of 1.8%, with J_{sc} = 4.9 mA/cm², V_{oc} = 0.92 V, and FF = 0.41, indicating that star molecules not only have better solubility, but also higher efficiency than the corresponding linear molecules.

Experimental Section

Materials and Instruments. All chemicals were purchased from commercial suppliers and used without further purification. THF and Et₂O were distilled from sodium with benzophenone as an indicator under nitrogen atmosphere. Hexane and CH₂Cl₂ were distilled from CaH₂. Chloroform was distilled before use. 4,7-Dibromo-2,1,3-benzothiadiazole,²⁵ 4,5,6,7-tetra-bromo-2,1,3-benzothiadiazole,²⁶ 2-bromo-3-hexylthiophene,²⁷ Pd[PPh₃]₄,²⁸ and Pd[PTh₃]₃²⁹ were prepared according to literature procedures. All reactions were performed under an atmosphere of nitrogen and monitored by thin layer chromatography (TLC) on silica gel 60 F254 (Merck, 0.2 mm). Column chromatography was carried out on silica gel (200–300 mesh).

¹H and ¹³C NMR spectra were recorded on a Bruker DM 300 or AV 400 spectrometer in CDCl₃. Electronic absorption spectra were obtained on a SHIMADZU UV–visible spectrometer model UV-1601PC. Fluorescence spectra were recorded on a Varian FLR025. Elemental analyses were performed on a Flash EA 1112 analyzer. Thermal gravimetric analysis (TGA; Pyris 1 TGA) measurements were carried out under a nitrogen atmosphere at a heating rate of 10 °C/min. Atomic force microscopy (AFM) measurements were performed under ambient conditions using a Digital Instrument Multimode Nanoscope IIIA operating in tapping mode. HOMO levels of all molecules synthesized in this study were determined by the ultraviolet photoelectron spectroscopy (UPS) measurements of a bulk thin film spin-coated on ITO. UPS characterizations (binding energy error of about 100 meV) were carried out with monochromatized HeI radiation at 21.2 eV in ultra high vacuum. The highest occupied molecular orbital (HOMO) values are here defined as the vertical ionization potential derived from UPS.

Fabrication and Characterization of OSCs. OSCs were fabricated with the device configuration of ITO/PEDOT:PSS/active layer/LiF/Al. The conductivity of ITO was 20 Ω/□ and PEDOT:PSS is Baytron AI 4083 from H. C. Starck. The ITO glass was cleaned, and a thin layer of PEDOT:PSS was spin coated at 3000 rpm/s and dried subsequently at 120 °C for 10 min on a hot plate and then transferred to a glovebox. The active layer was prepared by spin-coating the dichlorobenzene solution of molecules and PC₇₁BM on the top of ITO/PEDOT:PSS. Compounds **1-D**, **1-Q**, **2-D**, and **2-Q** are soluble in dichlorobenzene (DCB)

- (22) Cravino, A.; Leriche, P.; Alévêque, O.; Roquet, S.; Roncali, J. *Adv. Mater.* **2006**, *18*, 3033.
 (23) Roquet, S.; Cravino, A.; Leriche, P.; Alévêque, O.; Frère, P.; Roncali, J. *J. Am. Chem. Soc.* **2006**, *128*, 3459.
 (24) Wu, G. L.; Zhao, G. J.; He, C.; Zhang, J.; He, Q. G.; Chen, X. M.; Li, Y. F. *Sol. Energ. Mat. Sol. Cells.* **2009**, *93*, 108.

- (25) Ozyurt, F.; Gunbas, E. G.; Durmus, A.; Toppare, L. *Org. Electron.* **2008**, *9*, 296.
 (26) Bublitz, D. E. *J. Hetero. Chem.* **1972**, *9*, 539.
 (27) Chen, T. A.; Wu, X. M.; Rieke, R. D. *J. Am. Chem. Soc.* **1995**, *117*, 233.
 (28) Coulson, D. R. *Inorg. Synth.* **1972**, *13*, 121.
 (29) Li, W. W.; Han, Y.; Li, B. S.; Liu, C. M.; Bo, Z. S. *J. Polym. Sci., Part A: Polym. Chem.* **2008**, *46*, 4556.

when solutions were heated to 90 °C, so it is necessary to spin-coat active layers from DCB solution at elevated temperature. The resulting film was covered with a thermally evaporated 0.6 nm LiF layer, and subsequently 80 nm of aluminum, at a pressure of 10^{-6} Torr through a mask. The configurations of the solar cells are the same as in ref 3. Four OSCs were fabricated on one substrate, and the effective area of one cell is the overlap between two electrodes, which is in the range of 4–6 mm². Current–voltage characteristics were recorded using a Keithley 2400 Source meter under illumination of AM 1.5 with an intensity of 100 mW cm⁻² from a solar simulator (Model SS-50A, photo Emission Tech., Inc.).

***N,N*-Diphenyl-4-(thiophen-2-yl)benzenamine (1).** A mixture of 4,4,5,5-tetramethyl-2-(thiophen-2-yl)-1,3,2-dioxaborolane (4.00 g, 19.05 mmol), 4-bromo-*N,N*-diphenylbenzenamine (5.61 g, 17.28 mmol), THF (50 mL), water (10 mL), NaHCO₃ (15.1 g, 0.18 mol), and Pd(PPh₃)₄ (196 mg, 0.17 mmol) was carefully degassed and charged with nitrogen. The mixture was stirred and refluxed under N₂ for 48 h. CH₂Cl₂ was then added; the organic layer was separated; the aqueous layer was extracted with CH₂Cl₂; and the combined organic layers were dried over anhydrous Na₂SO₄ and evaporated to dryness. The residue was chromatographically purified on silica gel eluting with hexane/CH₂Cl₂ (6:1) to afford **1** as a yellow solid (2.88 g, 51%). ¹H NMR (400 MHz, CDCl₃) δ 7.46 (m, 2H), 7.24 (m, 6H), 7.10 (m, 9H). ¹³C NMR (400 MHz, CDCl₃) δ 147.59, 147.28, 144.34, 129.41, 128.64, 128.08, 126.83, 124.53, 124.10, 123.88, 123.13, 122.33. Anal. Calcd. for C₂₂H₁₇NS: C, 80.70; H, 5.23; N, 4.28. Found: C, 80.85; H, 5.23; N, 4.34.

***N,N*-Diphenyl-4-(5-(thiophen-2-yl)thiophen-2-yl)benzenamine (2).** A mixture of 2-(5-bromothiophen-2-yl)thiophene (5.04 g, 22.03 mmol), 4-(4,4,5,5-tetramethyl-1,3,2-dioxaborolan-2-yl)-*N,N*-diphenylbenzenamine (8.18 g, 22.03 mmol), THF (50 mL), water (10 mL), NaHCO₃ (18.5 g, 0.22 mol), and Pd(PPh₃)₄ (254 mg, 0.22 mmol) was carefully degassed and charged with nitrogen. The reaction mixture was stirred and refluxed under N₂ for 48 h. CH₂Cl₂ was then added; the organic layer was separated; the aqueous layer was extracted with CH₂Cl₂; and the combined organic layers were dried over Na₂SO₄ and evaporated to dryness. The residue was chromatographically purified on silica gel eluting with hexane/CH₂Cl₂ (4:1) to afford **2** as a yellow solid (6.36 g, 71%). ¹H NMR (400 MHz, CDCl₃) δ 7.51 (s, 1H), 7.49 (s, 1H), 7.31 (t, 4H), 7.22 (m, 2H), 7.17 (m, 6H), 7.12–7.03 (m, 5H). ¹³C NMR (100 MHz, CDCl₃) δ 147.47, 147.37, 143.07, 137.62, 135.85, 129.38, 128.10, 127.88, 126.43, 124.66, 124.59, 124.19, 123.65, 123.44, 123.20, 122.85.

4-(3-Hexylthiophen-2-yl)-*N,N*-diphenylbenzenamine (3). A mixture of 2-bromo-3-hexylthiophene (4 g, 16.2 mmol), 4-(4,4,5,5-tetramethyl-1,3,2-dioxaborolan-2-yl)-*N,N*-diphenylbenzenamine (7.2 g, 19.4 mmol), THF (50 mL), water (10 mL), NaHCO₃ (13.4 g, 0.16 mol), and Pd(PPh₃)₄ (185 mg, 0.16 mmol) was carefully degassed and charged with nitrogen. The reaction mixture was stirred and refluxed under N₂ for 48 h. CH₂Cl₂ was then added; the organic layer was separated; the aqueous layer was extracted with CH₂Cl₂; and the combined organic layers were dried over Na₂SO₄ and evaporated to dryness. The residue was chromatographically purified on silica gel eluting with hexane/CH₂Cl₂ (6:1) to afford **3** as a yellow solid (5.51 g, 83%). ¹H NMR (400 MHz, CDCl₃) δ 7.33 (m, 6H), 7.20 (m, 5H), 7.18 (m, 2H), 7.10 (m, 2H), 7.00 (d, 1H), 2.72 (t, 2H), 1.75 (m, 2H), 1.34 (m, 6H), 0.94 (t, 3H). ¹³C NMR (100 MHz, CDCl₃) δ 147.52, 146.89, 138.10, 137.60, 129.93, 129.41, 129.21, 128.58, 124.49, 123.10, 122.96, 31.56, 30.91, 29.07, 28.62, 22.51, 14.01. Anal. Calcd. for C₂₈H₂₉NS: C, 81.71; H, 7.10; N, 3.40. Found: C, 81.46; H, 7.37; N, 3.52.

4-(3-Hexyl-5-(4,4,5,5-tetramethyl-1,3,2-dioxaborolan-2-yl)thiophen-2-yl)-*N,N*-diphenylbenzenamine (5). To a solution of **3** (1 g, 2.43 mmol) in THF (50 mL) was added dropwise *n*-BuLi (1.17 mL, 2.5 mol/L in *n*-hexane) at –78 °C under nitrogen. The reaction was kept at –78 °C for 1 h. Then tri-*iso*-propyl borate (1.12 mL, 4.86 mmol) was added. The mixture was allowed to warm to room temperature overnight, and aqueous hydrochloric acid was added. The organic layer separated; the aqueous layer was extracted with ether; and the combined organic layers were dried over anhydrous Na₂SO₄ and evaporated to dryness. The residue was chromatographically purified on silica gel eluting with CH₂Cl₂ increasing to CH₂Cl₂/THF (10:1) to afford the boronic acid as a yellow liquid. A mixture of the obtained boronic acid, pinacol (1.6 g, 14 mmol), and dry CH₂Cl₂ was stirred and refluxed for 4 h. After the removal of the solvent, the residue was purified by chromatography on silica gel eluting with hexane/ethyl acetate (20:1) to afford **5** as a yellow solid (0.91 g, 70%). ¹H NMR (400 MHz, CDCl₃) δ 7.55 (m, 1H), 7.33 (m, 6H), 7.17 (m, 4H), 7.08 (m, 4H), 2.69 (m, 2H), 1.66 (m, 2H), 1.38 (s, 12H), 1.30 (m, 6H), 0.90 (t, 3H). ¹³C NMR (100 MHz, CDCl₃) δ 147.42, 147.15, 145.16, 139.80, 139.64, 129.73, 129.21, 128.35, 124.63, 123.07, 122.75, 83.85, 31.51, 30.86, 29.08, 28.58, 24.67, 22.45, 13.98. Anal. Calcd. for C₃₄H₄₀BNO₂S: C, 75.97; H, 7.50; N, 2.61. Found: C, 75.40; H, 7.43; N, 2.67.

4-(3-Hexyl-5-(3-hexylthiophen-2-yl)thiophen-2-yl)-*N,N*-diphenylbenzenamine (4). A mixture of 2-bromo-3-hexylthiophene (1.17 g, 4.74 mmol), **5** (3.05 g, 5.69 mmol), THF (20 mL), water (3 mL), NaHCO₃ (4 g, 47.6 mmol), and Pd(PPh₃)₃ (20 mg, 0.017 mmol) was carefully degassed and charged with nitrogen. The reaction mixture was stirred and refluxed under N₂ for 48 h. CH₂Cl₂ was added; the organic layer was separated; the aqueous layer was extracted with CH₂Cl₂; and the combined organic layers were dried over anhydrous Na₂SO₄ and evaporated to dryness. The residue was chromatographically purified on silica gel eluting with hexane/CH₂Cl₂ (3:1) to afford **4** as a yellow oil (2.51 g, 92%). ¹H NMR (400 MHz, CDCl₃) δ 7.35 (m, 3H), 7.29 (m, 3H), 7.15 (m, 7H), 7.07 (t, 2H), 7.02 (s, 1H), 6.95 (d, 1H), 2.84 (t, 2H), 2.71 (t, 2H), 1.68 (m, 4H), 1.35 (m, 12H), 0.92 (m, 6H). ¹³C NMR (100 MHz, CDCl₃) δ 147.46, 146.94, 139.10, 138.35, 137.52, 133.58, 130.88, 129.88, 129.73, 129.20, 128.27, 128.12, 124.52, 123.13, 123.01, 123.00, 31.58, 31.55, 30.80, 30.59, 29.16, 29.13, 29.06, 28.70, 22.52, 22.49, 13.98. Anal. Calcd. for C₃₈H₄₃NS₂: C, 78.98; H, 7.50; N, 2.42. Found: C, 78.26; H, 7.61; N, 2.49.

General Procedure for the Synthesis of Stannyl-Contained Compounds (1-Sn, 2-Sn, 3-Sn, and 4-Sn). To a solution of **1**, **2**, **3**, or **4** (1 mmol) in THF (50 mL) was added dropwise *n*-BuLi (1.2 mmol, 2.5 M in hexane) at –78 °C under nitrogen. The reaction was kept at –78 °C for 1 h. Then tributylchlorostannane (1.2 mmol) was added. The mixture was allowed to warm to room temperature overnight, and it was poured into water (100 mL). The organic layer was separated; the aqueous layer was extracted with ether; and the combined organic layers were dried over anhydrous Na₂SO₄ and evaporated to dryness. The residue was chromatographically purified on silica gel eluting with *n*-hexane/triethylamine (10:1, v:v) to afford the products (**1-Sn**, **2-Sn**, **3-Sn**, and **4-Sn**) as a yellow oil, which were used for the following reactions without further purification.

General Procedure for the Syntheses of 1, 2, 3, 4-D and 1, 2, 3, 4-Q by Stille Cross-Coupling Reaction. A mixture of 4,7-dibromo-2,1,3-benzothiadiazole (or 4,5,6,7-tetrabromo-2,1,3-benzothiadiazole) and stannyl derivative (**1-Sn**, **2-Sn**, **3-Sn**, or **4-Sn**) in toluene (20 mL) was carefully degassed before and after Pd[PPh₃]₄ was added. The mixture was heated at reflux, stirred under nitrogen for 24 h, and then allowed to cool to room

temperature. The mixture was poured into a large amount of methanol, and the resulting precipitate was collected by filtration. The crude product was subjected to Soxhlet extraction with methanol for 2 days and chromatographically purified on silica gel eluting with *n*-hexane/CH₂Cl₂ to afford the title compounds as dark solids. Compounds used for the solar cell device fabrication were further dissolved into a small amount of toluene, precipitated into a large amount of methanol, collected by filtration, and dried in high vacuum.

1-D. 4,7-Dibromo-2,1,3-benzothiadiazole (0.25 g, 0.85 mmol), **1-Sn** (1.8 g, 2.92 mmol), toluene (20 mL), and Pd[PPh₃]₄ (9.8 mg, 8.4×10^{-3} mmol) were used to afford **1-D** as a dark solid (0.44 g, 66%). ¹H NMR (400 MHz, CDCl₃) δ 8.09 (s, 2H), 7.83 (s, 2H), 7.55 (m, 4H), 7.27 (m, 10H), 7.14 (m, 16H). ¹³C NMR (100 MHz, CDCl₃) δ 147.52, 129.46, 128.79, 126.72, 124.83, 124.75, 123.58, 123.33. Anal. Calcd. for C₅₀H₃₄N₄S₃: C, 76.30; H, 4.35; N, 7.12. Found: C, 75.62; H, 4.32; N, 7.02. MALDI-TOF, *m/z*: Calcd, 786.2; Found, 786.5 (M⁺).

2-D. 4,7-Dibromo-2,1,3-benzothiadiazole (0.20 g, 0.68 mmol), **2-Sn** (1.8 g, 2.57 mmol), toluene (20 mL), and Pd[PPh₃]₄ (15.7 mg, 13.6×10^{-3} mmol) were used. A 0.39 g portion (a yield of 60%) of **2-D** was obtained. ¹H NMR (400 MHz, CDCl₃) δ 8.04 (s, 2H), 7.84 (s, 2H), 7.47 (m, 4H), 7.28 (m, 8H), 7.14 (m, 12H), 7.06 (m, 8H). Anal. Calcd. for C₅₀H₃₄N₄S₃: C, 73.23; H, 4.03; N, 5.89. Found: C, 73.60; H, 4.03; N, 5.91. MALDI-TOF, *m/z*: Calcd, 950.2; Found, 950.5 (M⁺).

3-D. 4,7-Dibromo-2,1,3-benzothiadiazole (0.14 g, 0.48 mmol), **3-Sn** (1 g, 1.43 mmol), toluene (20 mL), and Pd[PPh₃]₄ (5.5 mg, 4.8×10^{-3} mmol) were used. A 0.26 g portion (a yield of 56%) of **3-D** was obtained. ¹H NMR (400 MHz, CDCl₃) δ 8.02 (s, 2H), 7.80 (s, 2H), 7.39 (m, 4H), 7.30 (m, 8H), 7.17 (m, 8H), 7.12 (m, 4H), 7.05 (m, 4H), 2.78 (m, 4H), 1.73 (m, 4H), 1.33 (m, 12H), 0.90 (m, 6H). ¹³C NMR (100 MHz, CDCl₃) δ 152.49, 147.38, 147.36, 147.31, 147.22, 147.11, 139.24, 130.17, 129.74, 129.19, 128.08, 125.45, 124.97, 124.60, 123.07, 122.93, 31.54, 30.89, 29.12, 28.87, 22.50, 13.99. MALDI-TOF, *m/z*: Calcd, 955.4; Found, 954.4 (M⁺).

4-D. 4,7-Dibromo-2,1,3-benzothiadiazole (0.17 g, 0.58 mmol), **4-Sn** (1.2 g, 1.38 mmol), toluene (20 mL), and Pd[PPh₃]₄ (6.6 mg, 5.8×10^{-3} mmol) were used. A 0.44 g portion (a yield of 59%) of **4-D** was obtained. ¹H NMR (400 MHz, CDCl₃) δ 7.96 (s, 2H), 7.73 (s, 2H), 7.32 (m, 12H), 7.10 (broad, 18H), 2.89 (m, 4H), 2.73 (m, 4H), 1.75 (m, 8H), 1.38 (m, 24H), 0.94 (m, 12H). ¹³C NMR (100 MHz, CDCl₃) δ 152.59, 152.56, 147.68, 147.24, 140.11, 140.07, 133.74, 133.70, 130.87, 130.83, 130.03, 129.97, 129.88, 129.48, 128.24, 125.15, 125.08, 124.92, 123.31, 123.24, 123.70, 31.92, 31.88, 31.13, 30.74, 29.86, 29.59, 29.54, 29.43, 29.41, 29.05, 29.03, 22.87, 22.83, 22.79, 14.32, 14.31, 14.30. Anal. Calcd. for C₈₂H₈₆N₄S₅: C, 76.47; H, 6.73; N, 4.35. Found: C, 76.21; H, 6.69; N, 4.26. MALDI-TOF, *m/z*: Calcd, 1286.6; Found, 1286.6 (M⁺).

1-Q. Tetrabromo-2,1,3-benzothiadiazole (0.1 g, 0.22 mmol), **1-Sn** (0.81 g, 1.32 mmol), toluene (20 mL), and Pd[PPh₃]₄ (10 mg, 8.8×10^{-3} mmol) were used. A 0.27 g portion (a yield of 85%) of **1-Q** was obtained. ¹H NMR (400 MHz, CDCl₃) δ 7.47 (m, 6H), 7.41 (m, 4H), 7.28 (m, 14H), 7.17 (m, 18H), 7.05 (m, 18H), 6.83 (m, 4H). ¹³C NMR (100 MHz, CDCl₃) δ 153.84, 147.36, 147.27, 147.12, 146.61, 146.12, 138.07, 138.04, 135.83, 135.31, 131.95, 131.90, 131.40, 129.24, 128.19, 127.30, 126.61, 126.43, 124.46, 124.36, 123.58, 123.46, 123.04, 123.00, 121.91, 121.84. Anal. Calcd. for C₉₄H₆₄N₆S₅: C, 78.52; H, 4.49; N, 5.84. Found: C, 77.85; H, 4.54; N, 5.79. MALDI-TOF, *m/z*: Calcd, 1436.4; Found, 1437.5 (M⁺).

2-Q. Tetrabromo-2,1,3-benzothiadiazole (0.1 g, 0.22 mmol), **2-Sn** (0.92 g, 1.32 mmol), toluene (20 mL), and Pd[PPh₃]₄ (10 mg, 8.8×10^{-3} mmol) were used. 0.31 g (a yield of 80%) of **2-Q** was obtained. ¹H NMR (400 MHz, CDCl₃) δ 7.47 (m, 10H), 7.35 (m, 18H), 7.21 (m, 14H), 7.11 (m, 28H), 6.82 (m, 2H). ¹³C NMR (100 MHz, CDCl₃) δ 153.97, 147.70, 147.60, 147.57, 143.68, 143.47, 140.63, 140.30, 135.79, 135.73, 129.63, 128.30, 126.69, 125.27, 125.16, 124.85, 123.87, 123.80, 123.45, 123.34, 123.23, 123.13. MALDI-TOF, *m/z*: Calcd, 1764.3; Found, 1765.7 (M⁺).

3-Q. Tetrabromo-2,1,3-benzothiadiazole (60 mg, 0.13 mmol), **3-Sn** (0.55 g, 0.78 mmol), toluene (20 mL), and Pd[PPh₃]₄ (6.1 mg, 5.2×10^{-3} mmol) were used. 0.22 g (a yield of 93%) of **3-Q** was obtained. ¹H NMR (400 MHz, CDCl₃) δ 7.38–7.06 (m, 58H), 6.75 (s, 2H), 2.72 (t, 4H), 2.62 (t, 4H), 1.63 (m, 4H), 1.53 (m, 4H), 1.40–1.20 (m, 24H), 0.90 (m, 12H). ¹³C NMR (100 MHz, CDCl₃) δ 153.81, 147.50, 146.90, 146.82, 140.45, 139.67, 137.71, 137.56, 135.74, 134.87, 133.40, 129.79, 129.20, 128.50, 128.45, 126.90, 124.49, 124.42, 123.14, 123.08, 122.96, 122.94, 31.57, 31.25, 30.87, 29.07, 29.03, 28.98, 28.74, 28.56, 22.53, 22.48, 14.06. Anal. Calcd. for C₁₁₈H₁₁₂N₆S₅: C, 79.87; H, 6.36; N, 4.74. Found: C, 79.46; H, 6.50; N, 4.72. MALDI-TOF, *m/z*: Calcd, 1772.8; Found, 1773.8 (M⁺).

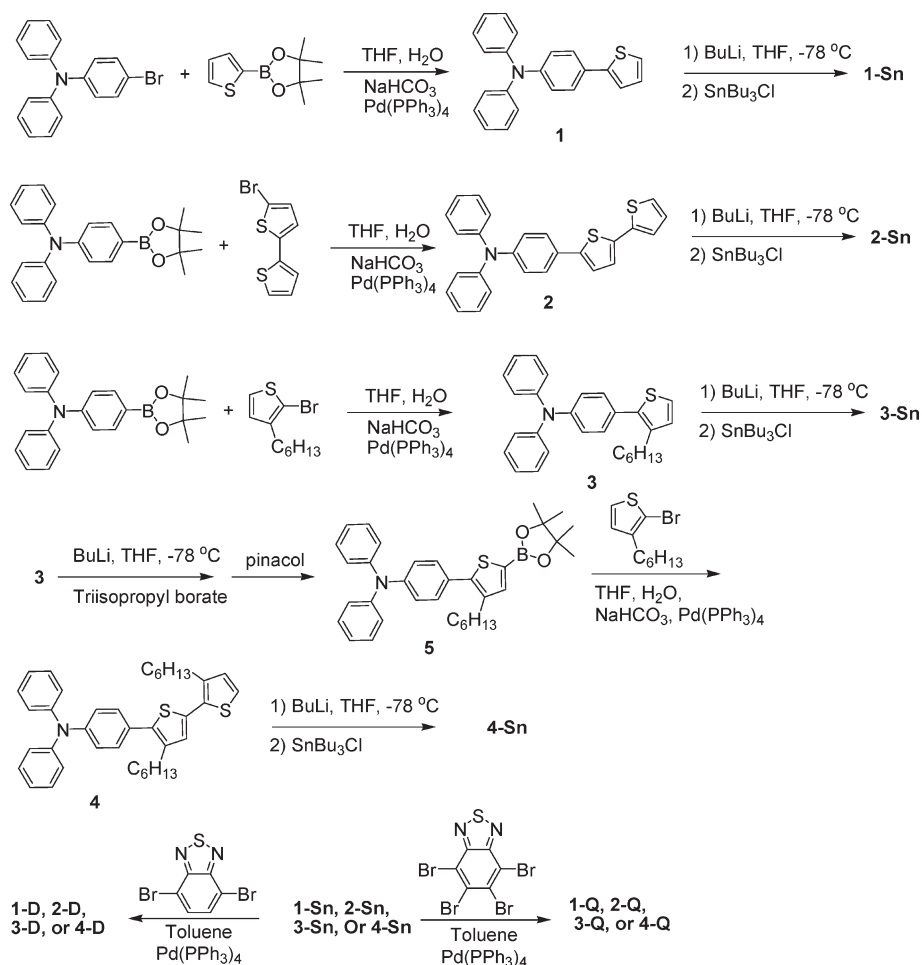
4-Q. Tetrabromo-2,1,3-benzothiadiazole (0.1 g, 0.22 mmol), **4-Sn** (1.1 g, 1.32 mmol), toluene (20 mL), and Pd[PPh₃]₄ (10 mg, 8.8×10^{-3} mmol) were used. 0.39 g (a yield of 73%) of **4-Q** was obtained. ¹H NMR (400 MHz, CDCl₃) δ 7.39–7.30 (m, 24H), 7.21–7.07 (m, 36H), 6.97 (s, 2H), 6.73 (s, 2H), 2.73 (t, 4H), 2.70 (m, 12H), 1.68 (m, 16H), 1.32 (m, 48H), 0.93 (m, 24H). ¹³C NMR (100 MHz, CDCl₃) δ 153.90, 147.73, 147.19, 147.15, 139.12, 138.72, 138.69, 138.62, 137.80, 134.30, 133.66, 133.34, 129.97, 129.95, 129.47, 128.48, 128.46, 124.78, 124.76, 123.32, 123.27, 123.25, 31.86, 31.82, 31.78, 31.14, 31.08, 30.74, 29.60, 29.44, 29.39, 29.35, 28.99, 22.82, 22.78, 14.32, 14.29, 14.27. Anal. Calcd. for C₁₅₈H₁₆₈N₆S₉: C, 77.79; H, 6.94; N, 3.44. Found: C, 77.71; H, 6.99; N, 3.45. MALDI-TOF, *m/z*: Calcd, 2437.1; Found, 2439.0 (M⁺).

Results and Discussions

Synthesis. The syntheses of D and Q series molecules are outlined in Scheme 1. Suzuki–Miyaura cross-coupling of 4-bromo-*N,N*-diphenylbenzenamine³⁰ and 4,4,5,5-tetramethyl-2-(thiophen-2-yl)-1,3,2-dioxaborolane²⁹ with Pd(PPh₃)₄ as the catalyst precursor afforded compound **1** in a yield of 51%. The treatment of compound **1** with *n*-BuLi at –78 °C followed by quenching with SnBu₃Cl to afford the desired **1-Sn** as a yellow oil, which was used for coupling reaction without further purification. Stille coupling of **1-Sn** with 4,7-dibromo-2,1,3-benzothiadiazole and 4,5,6,7-tetrabromo-2,1,3-benzothiadiazole with Pd(PPh₃)₄ as the catalyst precursor afforded compounds **1-D** and **1-Q** in yields of 66% and 85%, respectively. Following similar strategy, Suzuki–Miyaura cross-coupling of 4-(4,4,5,5-tetramethyl-1,3,2-dioxaborolan-2-yl)-*N,N*-diphenylbenzenamine and 2-(5-bromothiophen-2-yl)-thiophene afforded compound **2** in a yield of 71%. Compound **2-Sn** was obtained by treatment of compound **2** with *n*-BuLi at –78 °C followed by quenching with SnBu₃Cl. Stille coupling of compound **2-Sn** with

(30) Li, J. C.; Lee, H. Y.; Lee, S. H.; Zong, K.; Jin, S. H.; Lee, Y. S. *Synth. Met.* **2009**, *159*, 201.

Scheme 1. Synthesis Route of Linear and Star-Shaped Molecules



4,7-dibromo-2,1,3-benzothiadiazole and 4,5,6,7-tetrabromo-2,1,3-benzothiadiazole afforded compounds **2-D** and **2-Q** in yields of 60% and 80%, respectively. Suzuki–Miyaura coupling of 4-(4,4,5,5-tetramethyl-1,3,2-dioxaborolan-2-yl)-*N,N*-diphenylbenzenamine and 2-bromo-3-hexylthiophene, as above, afforded compound **3** in a yield of 83%. **3-Sn** was prepared from compound **3** using similar conditions as above. Similarly, the coupling of **3-Sn** with 4,7-dibromo-2,1,3-benzothiadiazole and 4,5,6,7-tetrabromo-2,1,3-benzothiadiazole gave compounds **3-D** and **3-Q** in yields of 56% and 93%, respectively. The treatment of compound **3** with *n*-BuLi at -78°C followed by quenching with tri-*iso*-propyl borate gave 5-(4-(diphenylamino)phenyl)-4-hexylthiophen-2-yl-2-boronic acid, which converted to compound **5** in a total yield of 70% by refluxing with pinacol in methylene chloride. Suzuki–Miyaura coupling of compound **5** and 2-bromo-3-hexylthiophene with $\text{Pd}(\text{PTh}_3)_3$ as the catalyst precursor furnished compound **4** in a yield of 92%. Following above procedures, compound **4** converted to compound 4-Sn. Coupling of compound **4-Sn** with 4,7-dibromo-2,1,3-benzothiadiazole and 4,5,6,7-tetrabromo-2,1,3-benzothiadiazole accomplished compounds **4-D** and **4-Q** in yields of 59% and 73%, respectively. ^1H and ^{13}C NMR spectroscopy, element analysis, and MALDI-TOF mass spectroscopy were used to characterize the structure

of these compounds. Thermogravimetric analysis (TGA) indicated that these molecules are stable up to about 300 °C. All molecules were dissolved in a small amount of toluene and then precipitated into a large amount of methanol, and the resulted precipitates were collected by filtration and dried in high vacuum to afford the desired product for OSCs.

Optical Properties. Optical absorption spectra of thin films of D-series and Q-series molecules are shown in Figure 2a and b. All molecules show two absorption bands in the range of 320–450 and 500–700 nm. The relative intensity of the band located at 320–450 nm is increased compared to the band at 500–700 nm for Q-series molecules, which is caused by the absorption of the two substituents at the 5 and 6 positions of benzothiadiazole. In tetrahydrofuran (THF) solution, the absorption peaks of these molecules are located at 500–700 nm, which are also summarized in Table 1 to compare with those of solid films. Noticeably, red shifts of absorption maxima in films for D-series and Q-series molecules are similar, both in the range of 16–36 nm. As shown in Table 1, Q-series molecules have much wider band gap and lower HOMO level than the corresponding D-series molecules. There are two thiophene units in the bridge of **2-D**, **4-D**, **2-Q**, and **4-Q**, as expected, their optical band gap is decreased, and the HOMO level is increased in

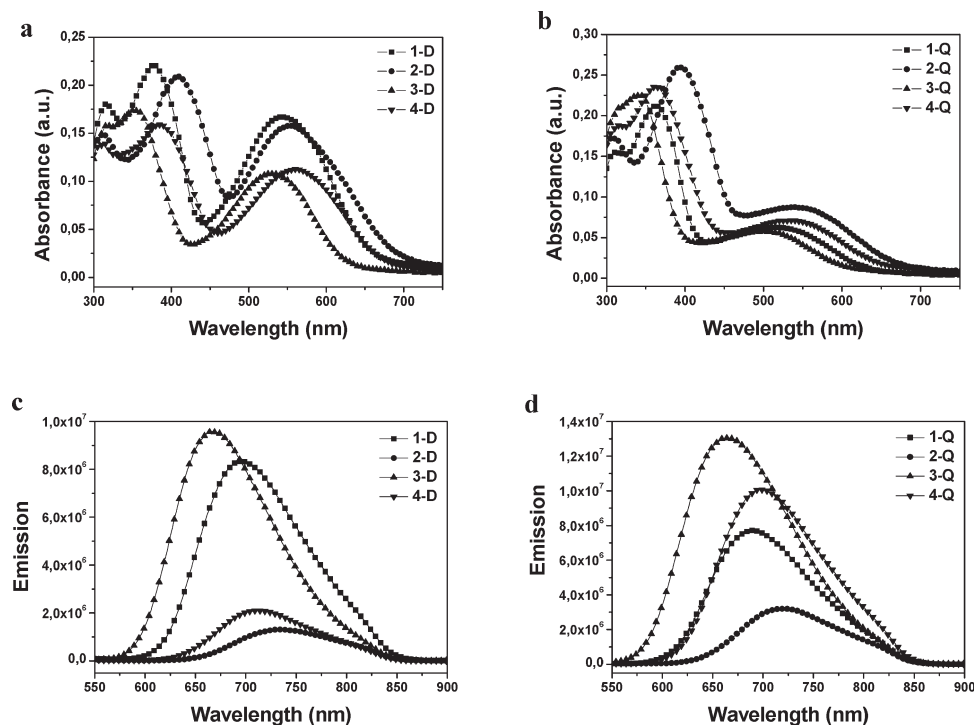


Figure 2. Absorption of small molecules (a) linear series and (b) star series and the PL spectra of small molecules (c) linear series and (d) star series in film.

Table 1. Summary of Absorption, Emission, Optical Bandgap, and HOMO Level of Linear and Star Molecules

com- pounds	absorption λ_{\max} solution	absorption λ_{\max} film	emission λ_{\max} (nm)	bandgap (eV)	HOMO ^a \pm 0.1 (eV)
1-D	533	553	696	1.85	-5.1
2-D	542	558	734	1.83	-5.1
3-D	514	530	668	1.98	-5.2
4-D	533	569	713	1.83	-5.0
1-Q	500	526	690	1.96	-5.45
2-Q	530	553	720	1.85	-5.3
3-Q	489	508	665	2.09	-5.4
4-Q	512	545	698	1.93	-5.3

^aThe HOMO level is measured by UPS.

comparison with those of **1-D**, **3-D**, **1-Q**, and **3-Q**. Therefore, the increasing of V_{oc} of OSCs can be achieved by the adjustment of the band gap and the HOMO level of molecules through the modification of their chemical structure.

Photoluminescence (PL) spectra of these molecules in thin films excited at 520 nm are also shown in Figure 2c and d and summarized in Table 1, in which emission peaks always locate at 660–740 nm as saturated red emission. There is no emission from blends of small molecules and PC₇₁BM excited at 520 nm, indicating efficient exciton dissociation in the blends.

Organic Solar Cells. Photovoltaic properties of these small molecules (D-series and Q-series) were investigated in devices with structure of ITO/PEDOT:PSS/active layer/LiF/Al, in which the active layer is composed with D-series or Q-series molecules as donors and PC₇₁BM as an acceptor. Solar cells were fabricated from DCB solutions, with heating spin-coating if needed. Different conditions were optimized, including ratio of donor to acceptor, thickness, and also additive. The optimized

performance were always achieved with the ratio of molecules to PC₇₁BM at 1:3 (w/w), except **2-D**, whose ratio is 1:2 (w/w). The thickness of the active layer is 70–90 nm. It has been proven that the additive 1,8-diiodooctane can improve the PCE of polymer solar cells,³¹ but there is nearly no improvement in these OSCs. The morphologies of the OSCs were imaged by AFM with an rms about 0.3 nm, as shown in Figure S1 in the Supporting Information.

The external quantum efficiencies (EQEs) of the OSCs based on D- and Q-series molecules blended with PC₇₁BM under monochromatic illumination are shown in Figure 3a and b. For both kinds of molecules, they exhibit similar EQEs, which are above 25% in visible region 400–700 nm and the peak is 38% for **3-Q** with an onset at 730 nm. The broad coverage of EQEs of these OSCs ensures a considerable J_{sc} .

The I - V characteristics of the OSCs were recorded under simulated solar illumination of AM 1.5 with an incident power density of 100 mW/cm² from -1 to +1 V and shown in Figure 4. The parameters of the OSCs are summarized in Table 2. Consistent with the HOMO levels in Table 1, the V_{oc} of the OSCs based on Q-series molecules is always larger than those of D-series molecules. FF is about 0.4, smaller than those of some polymers may be due to the short conjugated length and amorphous structures of the two series molecules. A large V_{oc} of 0.92 V combining with plausible J_{sc} of 4.9 mA/cm², the OSCs based on star molecule **3-Q** show a high PCE of 1.8%.

(31) Lee, J. K.; Ma, W. L.; Brabec, C. J.; Yuen, J.; Moon, J. S.; Kim, J. Y.; Lee, K.; Bazan, G. C.; Heeger, A. J. *J. Am. Chem. Soc.* **2008**, *130*, 3619.

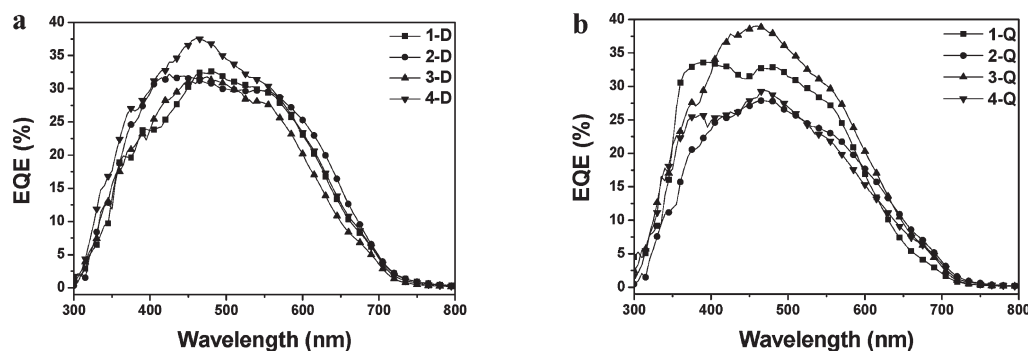


Figure 3. EQE of bulk heterojunction OSCs based on small molecules (a) D-series and (b) Q-series with PC₇₁BM under monochromatic illumination.

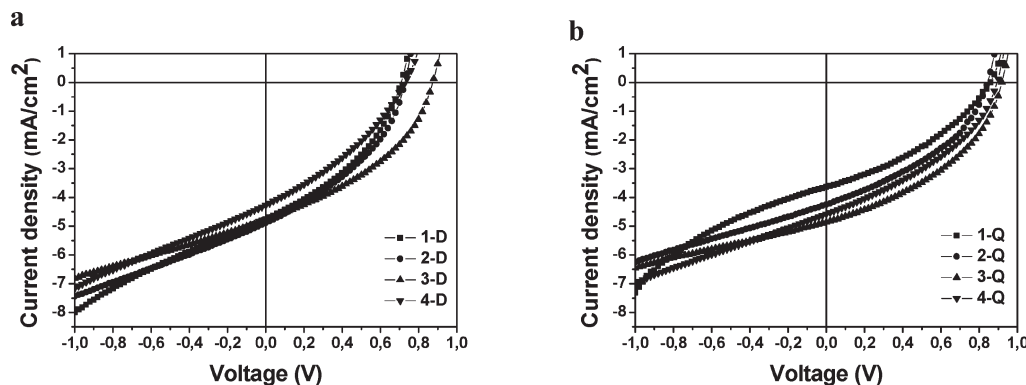


Figure 4. Current–voltage characteristics of OSCs based on small molecules and PC₇₁BM (a) D-series and (b) Q-series under AM 1.5 G illumination.

Table 2. Characteristic Properties of Small Molecule/PC₇₁BM Solar Cells

active layer	thickness [nm]	J_{sc} [mA/cm ²]	V_{oc} [V]	FF	PCE [%]
1-D/PC ₇₁ BM	75	4.8	0.71	0.38	1.3
2-D/PC ₇₁ BM	80	4.9	0.73	0.38	1.4
3-D/PC ₇₁ BM	70	4.8	0.87	0.40	1.7
4-D/PC ₇₁ BM	70	4.3	0.73	0.34	1.1
1-Q/PC ₇₁ BM	70	3.6	0.86	0.36	1.1
2-Q/PC ₇₁ BM	85	4.3	0.84	0.39	1.4
3-Q/PC ₇₁ BM	75	4.9	0.92	0.41	1.8
4-Q/PC ₇₁ BM	85	4.6	0.89	0.38	1.6

The performance of OSCs is mainly determined by free charge carrier generation, transport in the active layer, and collection at corresponding electrodes. The I – V characteristics of all the OSCs show strong electric field dependence (Figure 4), a typical feature of transport limitation. Small FFs (~ 0.4) of OSCs processing from solutions are due to large series resistance and small shunt resistance. AFM images of the blends (Figure S1 of the Supporting Information) present very smooth surfaces indicating fine mixture of two compounds, which may facilitate charge carrier recombination and result in large series resistance because of discontinuous paths for electrons and holes. The active layers of solution processed OSCs are generally not as dense as polymer films, which form texture structure by polymer chains. Less dense active layers of OSCs deteriorate FF through large leakage current or small shunt resistance. We noticed that the dark current could be significantly reduced with thick active layer; however, a thick active layer would increase series resistance, therefore, resulting in a smaller J_{sc} and

FF and lower PCE. Control of the morphology of blends to the desired phase separation and forming dense films may improve charge transport, depress leakage current, and, in turn, increase FF.

However, the large photocurrent (6 – 7 mA/cm²) under reverse bias of 1 V illustrates that a big amount of excitons could be produced and dissociated, which means the charge generation in the active layers does not hinder the performance of the OSCs. It is obvious that an electric field is needed to extract free charge carriers under current device conditions, which may be improved with preferred morphology or/and suitable electrodes with big work function difference. Potential large photocurrent combining with V_{oc} of 0.92 V makes the materials very promising for application in OSCs.

Conclusion

In conclusion, a series of soluble donor–acceptor–donor small molecules, D-series and Q-series, based on benzothiadiazole with linear and star structures have been synthesized via Stille-coupling reaction. The optical band gap of these small molecules is 1.8–2.1 eV, which is suitable for OSCs. OSCs have been fabricated from solution spin-coating with these soluble small molecules as donor and PC₇₁BM as acceptor. Star molecules have lower HOMO levels than the corresponding linear D-series molecules, resulting in high V_{oc} in OSCs. The results show that Q-series have higher efficiency than D-series due to their large V_{oc} . OSCs based on star molecule 3-Q show the highest PCE of 1.8%.

Acknowledgment. The work was conducted through the collaboration between Linköping University, Sweden, and Institute of Chemistry, Chinese Academy of Sciences, financed by Swedish Research Links Program of Swedish Research Council (VR). Financial support by the NSF of China (20834006 and 50821062) and the 863 Program (2008AA05Z425) is gratefully acknowledged. We thank

Prof. Olle Inganäs of Linköping University for providing the facility to conduct the research.

Supporting Information Available: AFM height images of the active elayers and $J-V$ characterization under illumination and in the dark. This material is available free of charge via the Internet at <http://pubs.acs.org>.